

Technical report 10-049

Variable speed limits for area-wide reduction of emissions*

S.K. Zegeye, B. De Schutter, J. Hellendoorn, and E.A. Breunese

If you want to cite this report, please use the following reference instead:

S.K. Zegeye, B. De Schutter, J. Hellendoorn, and E.A. Breunese, “Variable speed limits for area-wide reduction of emissions,” *Proceedings of the 13th International IEEE Conference on Intelligent Transportation Systems (ITSC 2010)*, Madeira Island, Portugal, pp. 507–512, Sept. 2010.

Delft Center for Systems and Control
Delft University of Technology
Mekelweg 2, 2628 CD Delft
The Netherlands
phone: +31-15-278.24.73 (secretary)
URL: <https://www.dcsc.tudelft.nl>

* This report can also be downloaded via https://pub.bartdeschutter.org/abs/10_049.html

Variable Speed Limits for Area-Wide Reduction of Emissions

S. K. Zegeye, B. De Schutter, J. Hellendoorn, and E. A. Breunese

Abstract—Although traffic congestion is a pressing problem that drivers face every day, improving the traffic flow does not always create a healthy environment to the people residing in the neighborhood of the freeway. Improved traffic flow neither means efficient fuel consumption of the vehicles. Moreover, reduction of total emissions or travel times in a traffic network does not always guarantee reduction in the area-wide emission levels, because there are many other factors that affect the area-wide emissions. In particular, the direction and speed of wind are important factors that play a significant role in the area-wide emission levels. Therefore, in this paper, we systematically model the effect of wind on the area-wide emission levels and design a model-based traffic controller to reduce the dispersion of emissions. More specifically, a model predictive control (MPC) is used to integrate various variable speed limits in order to provide a balanced trade-off between the area-wide emissions and the travel times. Furthermore, we present a case study to demonstrate the proposed control approach.

I. INTRODUCTION

Due to the continuous increase in the demand for mobility and transportation, traffic jams are occurring frequently in many traffic networks. The rise in fuel prices and the imposition of stringent environmental policies did not bring down the traffic demand to the level where a safer environment and improved traffic flows can be realized. Moreover, traffic jams also cause emissions and the related adverse effects on human health. Recent studies have shown that NO_2 has adverse health effects [11]. In most European cities, road traffic exhaust emissions account for more than 70% of NO_x [11]. Similarly, in the US road traffic exhaust emission contribute about 45% of the released pollutants [8].

There are several possible approaches to address these problems. One of the economically and environmentally sound solutions is the implementation of intelligent transportation systems [14]. In such systems different traffic control measures (such as variable speed limits, traffic signals, ramp metering, route guidance, etc.) are used to minimize the impact of traffic jams (such as longer travel times, increased emission levels, and fuel consumption) and to improve the safety of the traffic networks.

Although it has become a well known fact that an improved traffic flow does not prove reduced emissions nor efficient fuel consumption [1], [13], it is not yet clear how to efficiently control the traffic networks in such a way that a balanced trade-off between the demands of drivers,

transport authorities, and environmental bodies is obtained. Moreover, a traffic controller focusing on the reduction of emissions does not always guarantee reduced travel times or fuel consumption [13]. Furthermore, a traffic controller that could reduce the total emissions may cause intense dispersion of emissions levels in certain areas. To make matter worse, depending on the direction and speed of wind the same controller with the same objectives and the same traffic conditions can perform differently.

Moreover, although it is believed that the construction of additional freeways could reduce the frequency traffic jams in certain areas [8], transport authorities very often opt not to construct new infrastructure due to the environmental impact it may cause to some local areas. If one could design a traffic controller that can guarantee that certain maximum levels of area-wide emissions for targeted areas will not be exceeded, it may help to consider construction of strategic road networks without either displacing the vulnerable neighborhoods or affecting their environment.

We therefore design a controller and investigate its effect on the dispersion of emissions on a specific area. We model the effect of wind speed and direction on the levels of the area-wide emissions. We use a model-based control approach to reduce area-wide emissions while still improving the traffic flow. In particular, we implement Model Predictive Control (MPC) with a multi-objective function based on weighted sum of the total time spent (TTS), the total emissions (TE), and the maximum dispersion levels (MDL). We use variable speed limit control to improve the TTS, the TE, and the MDL. We also demonstrate the proposed control approach with a case study of a freeway network. The results show that the proposed control strategy can be used to provide a balanced trade-off between the various objectives.

A. The philosophy of model predictive control

The fundamental concept of Model Predictive Control (MPC) [10] lies in the optimization of control inputs based on prediction and a moving horizon approach. We consider both the system and the MPC controller in discrete time. A measurement of the system states is made every control time step. Using a model of the system and numerical optimization, the MPC controller determines a sequence of control inputs that optimize a performance criterion over a given future time horizon (i.e. from control step ℓ up to $\ell + N_p$ (see Fig. 1(b))). At each control time step ℓ , only the first sample of the optimal control input is applied to the system; afterward the time axis is shifted one control time step. Then, based on the new states and control inputs of the system, a

S. K. Zegeye, B. De Schutter, and J. Hellendoorn are with the Delft Center for Systems and Control, Delft University of Technology, Delft, The Netherlands. {s.k.zegeye,b.deschutter,j.hellendoorn}@tudelft.nl

E. A. Breunese is with Shell Nederland B.V. The Hague, The Netherlands. ewald.breunese@shell.com

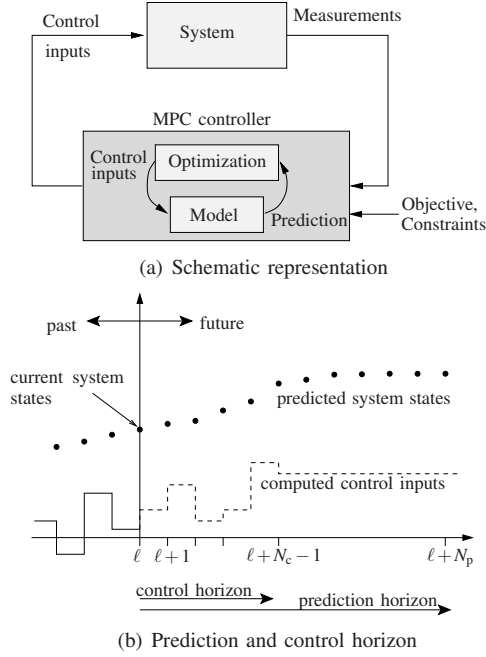


Fig. 1. Conceptual representation of model predictive control.

new sequence of optimal control input is generated. Once again the first control input is applied. At every control time step this process is repeated.

Fig. 1(a) illustrates the MPC concept. The system block represents the real system of which the states are measured every control step T_c . The MPC controller block contains the model of the system and an optimization tool. The MPC controller designs the control inputs in such a way that a given objective function is optimized. Fig. 1(b) depicts the concepts of prediction and control horizons, where it shows that the control inputs are kept constant after the control horizon $N_c \leq N_p$.

The main advantage of MPC is its ability to take constraints into account and that it can be used for nonlinear systems. Its main limitation emanates from the computation time required by the optimization process. To alleviate the computational problems several methods can be used (e.g. introducing a control horizon, blocking method, and parametrization of control inputs) [10], [6].

B. MPC for traffic flow and emission dispersion control

In MPC-based traffic control systems, the system in Fig. 1(a) represents the real traffic system to be controlled. Different sensors measure the speed, flow, density, etc. of the traffic system and feed it to the MPC controller at every control step T_c . The MPC controller uses models of the traffic system to predict the future evolution of the traffic flow and the effects of its control actions on the traffic performance measures (such as travel times, emissions, fuel consumptions, and area-wide emissions). In particular, in this paper we use macroscopic models of the traffic system. Some possible models that can be used are discussed in Sections II and III. Note, however, that the MPC control approach is generic and

it can also accommodate other, more complex traffic flow, emission, and area-wide emission models.

As objective function we could for example consider the following measure¹:

$$J(\ell) = \zeta_1 \frac{TTS(\ell)}{TTS_n} + \zeta_2 \frac{TE(\ell)}{TE_n} + \zeta_3 \frac{TFC(\ell)}{TFC_n} + \zeta_4 \frac{DL(\ell)}{DL_n} + \zeta_5 \frac{\Delta(\ell)}{\Delta_n} \quad (1)$$

where, $\zeta_n \geq 0$ for $n = 1, 2, 3, 4, 5$ are weighting coefficients, $TTS(\ell)$, $TE(\ell)$, $TFC(\ell)$, and $DL(\ell)$ are respectively the total time spent, the total emissions, the total fuel consumption, and the dispersion levels over the period $[\ell T_c, (\ell + N_p) T_c]$, $\Delta(\ell)$ denotes the change of the control input over time and space, and the subscript 'n' is used to denote the nominal values of the respective variables (i.e. the values of the variables obtained under nominal operation of the system, where no controller is implemented).

Unlike the TTS, TE, or TFC in (1), the definition of the dispersion level DL can vary depending on the intentions of the criterion. In some cases it may be important to focus only on the reduction of the maximum dispersion levels; in some other cases it can be equally or more important to reduce the cumulative exposure of an area to dispersion of emissions; or the combination of the two cases. Hence, depending on the regulations to be adopted the formulation of DL in (1) can be different. Some examples are:

$$DL(\ell) = \|D(\ell)\|_{\infty} \quad (2)$$

$$DL(\ell) = \delta_1 \|D(\ell)\|_{\infty} + \delta_2 \|D(\ell)\|_{1/2} \quad (3)$$

$$DL(\ell) = \|D(\ell)\|_{1/2} \quad \text{s.t. the additional constraint} \quad \|D(\ell)\|_{\infty} \leq DL_{\max} \quad (4)$$

$$DL(\ell) = \delta_1 \max(\|D(\ell)\|_{\infty} - DL_{\max}, 0) + \delta_2 \|D(\ell)\|_{1/2} \quad (5)$$

where $D(\ell)$ is a vector containing dispersion levels at consecutive sample time instants in the period $[\ell, N_p + \ell - 1]$, δ_1 and δ_2 denote weighting factors, the operator $\|x\|_{1/2}$ denotes the 1- or 2-norm of x , and DL_{\max} denotes the maximum dispersion level allowed.

The definition in (2) stresses the reduction of the maximum dispersion level. But it is also possible to augment the cumulative area-wide emissions as in (3), where the emphasis can be determined by the weighting factors. Another possible formulation which focuses on the reduction of the cumulative dispersion while limiting the maximum of the dispersion levels below certain predefined level is given in (4). However, due to the hard constraint on the maximum dispersion level, the resulting optimization problem may be infeasible for certain cases. The problem can be solved by relaxing the formulation as in (5).

C. Optimization method

One of the bottlenecks in MPC control approach is the extensive optimization and the resulting computational requirements. The MPC optimization problem considered for

¹MPC is generic as regards the choice of the performance criteria, and so other objective functions could also be considered instead.

this paper is nonlinear and nonconvex. Thus a proper choice of an optimization technique has to be made in order to obtain feasible optimal control values. Owing to the non-convex nature of the objective function, global, or multi-start local optimization methods are required. Hence, multi-start sequential quadratic programming [9, Section 5.3], pattern search [2], genetic algorithms [4], or simulated annealing [5] can be used.

II. TRAFFIC FLOW AND EMISSION MODELS

A. METANET

METANET [7] is a macroscopic second-order traffic flow model. The model describes the evolution of the traffic variables, viz. the density, the flow, and the space-mean speed, as a system of nonlinear difference equations. The METANET model is discrete both in time and space. Let T be the simulation step size and k be the simulation step counter². In the METANET model, a node is placed at a point where there is a change in the geometry of a freeway (such as a lane drop, an on/off-ramp, or a bifurcation). A homogeneous freeway that connects such nodes is called a link. Links are further divided into segments of length 500-1000 m [7]. The equations that describe the traffic dynamics in segment i of link m are given by

$$q_{m,i}(k) = \lambda_m \rho_{m,i}(k) v_{m,i}(k) \quad (6)$$

$$\rho_{m,i}(k+1) = \rho_{m,i}(k) + \frac{T}{L_m \lambda_m} [q_{m,i-1}(k) - q_{m,i}(k)] \quad (7)$$

$$v_{m,i}(k+1) = v_{m,i}(k) + \frac{T}{\tau} [V[\rho_{m,i}(k)] - v_{m,i}(k)] \\ + \frac{T v_{m,i}(k) [v_{m,i-1}(k) - v_{m,i}(k)]}{L_m} \\ - \frac{T \eta [\rho_{m,i+1}(k) - \rho_{m,i}(k)]}{\tau L_m (\rho_{m,i}(k) + \kappa)} \quad (8)$$

$$V[\rho_{m,i}(k)] = \min \left\{ (\alpha_m + 1) u_{m,i}(k), \right. \\ \left. v_{\text{free},m} \exp \left[-\frac{1}{a_m} \left(\frac{\rho_{m,i}(k)}{\rho_{\text{cr},m}} \right)^{a_m} \right] \right\} \quad (9)$$

where $q_{m,i}(k)$, $\rho_{m,i}(k)$, $v_{m,i}(k)$, and $u_{m,i}(k)$ denote respectively the flow, density, space-mean speed, and variable speed limit of segment i of link m at the simulation step k , L_m denotes the length of the segments of link m , and λ_m denotes the number of lanes of link m . Furthermore, $\rho_{\text{cr},m}$ is the critical density, τ a time constant, η the anticipation constant, a_m the parameter of the fundamental diagram, α_m the drivers' compliance factor, and κ is a model parameter.

For origins (such as on-ramps and mainstream entry points) a queue model is used. The dynamics of the queue length w_o at the origin o are modeled as

$$w_o(k+1) = w_o(k) + T(d_o(k) - q_o(k)) \quad (10)$$

²For the sake of simplicity we assume that the control step size T_c and the simulation step size T are related by $T_c = MT$, for some positive integer M . Therefore, at time $t = \ell T_c = kT$ the control step counter ℓ is an integer divisor of the simulation step counter k . They are then related by $k(\ell) = M\ell$.

where d_o and q_o denote respectively the demand and outflow of the origin o . The outflow q_o is given by

$$q_o(k) = \min \left[d_o(k) + \frac{w_o(k)}{T}, r_o(k) C_o, \right. \\ \left. C_o \left(\frac{\rho_{\text{jam},m} - \rho_{m,1}(k)}{\rho_{\text{jam},m} - \rho_{\text{cr},m}} \right) \right], \quad (11)$$

with $r_o(k)$ the ramp metering rate (where $r_o \in [0, 1]$ for a metered on-ramp and $r_o(k) = 1$ for an unmetered on-ramp or mainstream origin), $\rho_{\text{jam},m}$ the maximum density of link m , and C_o the capacity of the origin o .

B. VT-macro

The VT-macro model [12] is a macroscopic emission and fuel consumption model that we have in particular developed for the METANET traffic flow model. The model takes the dynamics of the average space-mean speed of the traffic flow model into account. The inputs of the VT-macro model are the average space-mean speed, average acceleration, and the number of vehicles subject to the speed and acceleration pairs. These variables are computed from the space-mean speed, density, and flow variables of the METANET model.

Mathematically, the VT-macro model can be compactly described as

$$J_{y,m,i}(k) = f(v_{m,i}(k), v_{m,i}(k+1), v_{m,i+1}(k+1), \rho_{m,i}(k)) \quad (12)$$

where $J_{y,m,i}(k)$ [kg/s] is the estimate or prediction of the variable $y \in \mathcal{Y} = \{\text{CO}, \text{NO}_x, \text{HC}, \text{CO}_2\}$ of segment i of link m during the time period $[kT, (k+1)T]$ and f is a nonlinear mapping (for detailed discussion we refer to [12]).

III. AREA-WIDE EMISSION MODELING

Dispersion of vehicular emissions in a traffic network is affected by several factors. The main factors are the speed of the vehicles, the weather conditions (such as rain, wind, and temperature), and the geometry of the freeway area. The speeds of the vehicles influence the dispersion of the emissions in the vicinity of the road [3]. In the region far from the road, where most residences, schools, and other buildings are located, the dispersion of the emissions is primarily dependent on the speed and direction of the wind and the temperature of the atmosphere [3].

In the sequel we model the dispersion of emissions (i.e. area-wide emissions) at a specific location at some distance from a traffic freeway. Since, the distance is considered to be large, the effect of the speed of the vehicles on the dispersion of the emissions is assumed to be negligible. Moreover, the wavefronts of the emissions are considered approximately planar at far distance from the road. The emissions are also assumed to emanate from the center point of the segments of the links introduced in Section II-A. This assumption is valid when the length of the freeway segment is much smaller than the distance from the segment to the target.

Fig. 2 depicts a 2D representation of the dispersion of the emissions. It shows a traffic flow from the West to the East on the freeway. The wind with speed V_w is directed at an angle $\varphi \in [0, 2\pi]$ with respect to the freeway. The area of the target

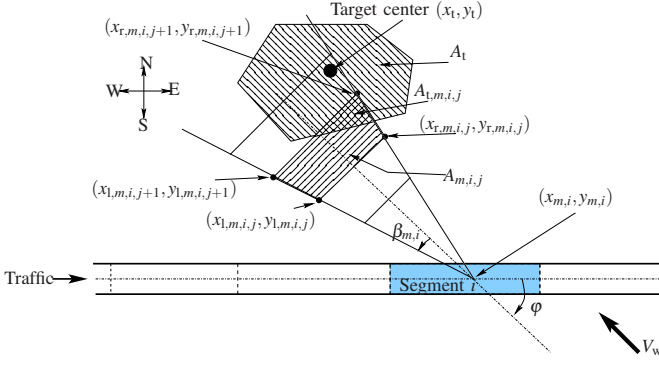


Fig. 2. 2D schematic diagram of area-wide emissions of vehicles in a segment of a link.

polytope P_t with geometric center (x_t, y_t) is denoted by A_t . The trapezoidal areas formed by the wavefronts emanating from the center point $(x_{m,i}, y_{m,i})$ show the direction and size of the dispersion level of the emissions $J_{y,m,i}$ (see (12)) from the vehicles in the segment i of link m in the direction of the wind. The emissions of segment i of link m (the j^{th} trapezoid $T_{m,i,j}$ formed by the wavefront of the segment) cover a region $P_{t,m,i,j}$ of the target P_t after a time delay of $d_{m,i,j}$ units. The time delay $d_{m,i,j}$ is defined as the number of time steps required by the wavefront of the dispersion of the emissions to reach the trapezoid formed by the vertices $(x_{l,m,i,j}, y_{l,m,i,j})$, $(x_{l,m,i,j+1}, y_{l,m,i,j+1})$, $(x_{r,m,i,j}, y_{r,m,i,j})$, and $(x_{r,m,i,j+1}, y_{r,m,i,j+1})$. The quantity $A_{m,i,j}$ denotes the area of the trapezoid $T_{m,i,j}$ formed by these vertices. The vertices are computed using the relations

$$\begin{aligned} x_{l,m,i,j} &= x_{m,i} - V_w T d_{m,i,j} \frac{\cos(\varphi - \beta_{m,i})}{\cos(\beta_{m,i})} \\ y_{l,m,i,j} &= y_{m,i} + V_w T d_{m,i,j} \frac{\sin(\varphi - \beta_{m,i})}{\cos(\beta_{m,i})} \\ x_{r,m,i,j} &= x_{m,i} - V_w T d_{m,i,j} \frac{\cos(\varphi + \beta_{m,i})}{\cos(\beta_{m,i})} \\ y_{r,m,i,j} &= y_{m,i} + V_w T d_{m,i,j} \frac{\sin(\varphi + \beta_{m,i})}{\cos(\beta_{m,i})} \end{aligned}$$

with the angle $\beta_{m,i}$ denoting the lateral divergence of the emissions as the emissions propagate in the horizontal direction of the wind.

Since the emissions get dispersed in all directions when the wind speed is zero, then the maximum lateral angle for a flat surrounding without any mountains or buildings is $\beta_{\max,m,i} = \pi$. Moreover, the angle gets smaller as the wind speed increases. Hence, we consider the relation of the angle to the wind speed to be as

$$\beta_{m,i} = \frac{\beta_{\max,m,i}}{1 + \beta_0 V_w} \quad (13)$$

where $\beta_0 > 1$ is model parameter.

In the vertical direction, we consider a vertical dispersion factor $0 < \gamma < 1$ such that the emissions are reduced by a factor γ at every time step. Thus, the emission levels at the

j^{th} trapezoid due to segment i of link m will be

$$J_{y,m,i,j}(k) = J_{y,m,i}(k - d_{m,i,j}) \gamma^{d_{m,i,j}-1} \quad (14)$$

where $J_{y,m,i}(k)$ is as defined in (12).

Note that the wavefront of the emission traverses a distance $V_w T$ (the height of the trapezoids) every simulation step size T in the direction of the wind V_w . Moreover, not all the trapezoids that are formed by the wavefronts intersect with the target area. Since the target polytope P_t and the trapezoids $T_{m,i,j}$ are bounded polytopes, the intersection of these areas $P_{t,m,i,j}$ is also a polytope. We denote the area of the $P_{t,m,i,j}$ by $A_{t,m,i,j}$. Hence, the emission contribution of segment i of link m over the target area is

$$J_{t,y,m,i}(k) = \sum_{j \in \mathcal{J}_{\text{all},m,i}} \frac{A_{t,m,i,j}}{A_{m,i,j}} J_{y,m,i,j}(k) \quad (15)$$

where $\mathcal{J}_{\text{all},m,i}$ is the set of all trapezoids formed by the wavefronts of segment i of link m and that intersect the target polytope P_t .

Thus, the total emission density at the target area over the period $[kT, (k+1)T]$ will be

$$J_{D,t,y}(k) = \frac{1}{A_t} \sum_{(m,i) \in \mathcal{J}_{\text{Emi}}} J_{t,y,m,i}(k) \quad (16)$$

where \mathcal{J}_{Emi} is the set of all segments of links that contribute emissions to the target area.

Unlike the linear dispersion models, this point source dispersion model does not require numerical integral computations, and hence it is suitable for on-line predictions.

IV. CASE STUDY

In the sequel we present the case study considered to illustrate the control approach presented in Section I-A and the models described in Section II and III.

A. Freeway scenario

We consider a 12 km freeway stretch which is sectioned into twelve equal segments of size 1 km. Each section of the freeway is equipped with a variable speed limit control (see Fig. 3). The speed limit are coupled in groups of four, where each group displays the same speed limit at the same time. We assume a school with an area of $200 \text{ m} \times 200 \text{ m}$ located 2 km north and 6 km east of the origin of the freeway (i.e. $(x_t, y_t) = (6 \text{ km}, 2 \text{ km})$). We further consider wind blowing with speed $V_w = 8 \text{ m/s}$ and in the north-west direction of the freeway with an angle $\varphi = \pi/3$ with respect to the freeway (see Fig. 3).

B. Performance criteria

We consider a multi-objective performance criterion that accommodates the emissions, dispersion of emissions, and travel time. The multi-objective function is defined as a weighted sum of the three objectives similar to (1). In particular, we consider the objective function given by

$$J(\ell) = \zeta_1 \frac{\text{TTS}(\ell)}{\text{TTS}_n} + \zeta_2 \frac{\text{TE}(\ell)}{\text{TE}_n} + \zeta_3 \frac{\text{DL}(\ell)}{\text{DL}_n} + \zeta_4 \frac{\Delta(\ell)}{\Delta_n} \quad (17)$$

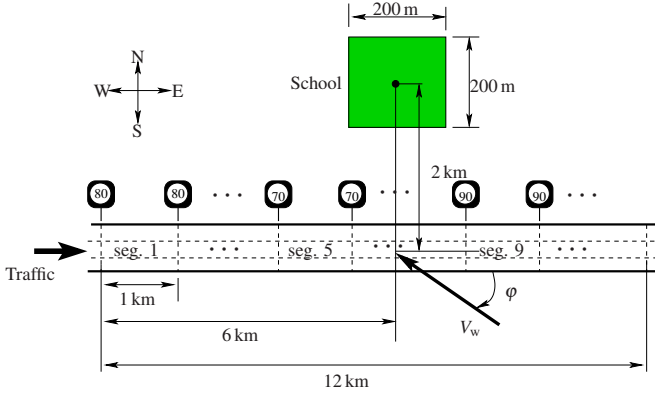


Fig. 3. Traffic freeway considered for the case study.

where

$$\begin{aligned} \text{TTS}(\ell) &= T \sum_{k=M\ell}^{MN_p-1} \sum_{(m,i) \in \mathcal{S}_{\text{all}}} \lambda_m L_m \rho_{m,i}(k) \\ &\quad + T \sum_{k=M\ell}^{MN_p-1} \sum_{o \in \mathcal{O}_{\text{all}}} w_o(k), \\ \text{TE}(\ell) &= \sum_{y \in \mathcal{Y}} \mu_y \frac{\text{TE}_y(\ell)}{\text{TE}_{y,n}}, \quad \text{DL}(\ell) = \sum_{y \in \mathcal{Y}} \mu_y \frac{\text{DL}_y(\ell)}{\text{DL}_{y,n}}, \\ \Delta(\ell) &= \sum_{k=M\ell}^{MN_p-1} \sum_{s \in \mathcal{S}_{\text{all}}} \left(\|u_s(k) - u_s(k-1)\|_2^2 \right. \\ &\quad \left. + \|u_s(k) - u_{s-1}(k)\|_2^2 \right), \end{aligned}$$

with

$$\begin{aligned} \text{TE}_y(\ell) &= \sum_{k=M\ell}^{MN_p-1} \sum_{(m,i) \in \mathcal{S}_{\text{all}}} J_{y,m,i}(k), \\ \text{DL}_y(\ell) &= \|[J_{D,t,y}(M\ell) \dots J_{D,t,y}(MN_p-1)]^\top\|_\infty, \end{aligned}$$

μ_y denoting the weightings of the emissions $y \in \mathcal{Y}$ (in particular we consider $\mu_y = 1$), and \mathcal{S}_{all} and \mathcal{O}_{all} denoting respectively the set all segments of links and the set of all origins in the traffic network and \mathcal{S}_{all} denoting the set of all speed limits. Moreover, the nominal values of the TTS, TE, TE_y , DL, DL_y , and Δ_n are computed by simulating the uncontrolled traffic system with all speed limits set to 80 km/h.

C. Results and discussion

We simulate the evolution of the case study over 1 h. The simulation results for different combinations of the TTS, TE, and DL weights are tabulated in Table I. Note that the fluctuation in the control input (Δ) is weighted smaller ($\zeta_4 = 0.01$) than either of TTS, TE, or DL, because the main intent of the controller is to reduce either of TTS, TE, or DL, while also reducing Δ with a lesser degree of importance. The first row of the table shows the results of the simulation for a case where no controller is implemented. The evolution of

the dispersion of the emissions of the freeway of the case study on the school area is depicted in Fig. 4.

The evolution of the dispersion levels in Fig. 4 have the same initial value in all cases. This is because the initial emission levels of the freeway cannot be affected by the controller. Hence, only the impact of the emissions emitted after the start of the simulation can be affected.

When the objective of the controller is to reduce the TTS (with the weighting vector $\zeta = [1 \ 0 \ 0 \ 0.01]$), the dispersion level is smaller than in the uncontrolled case only for about 15 min. However, after about 30 min of the simulation time, the dispersion level of the TTS controlled case on the target area becomes higher for the rest of the simulation time. As a result, in Table I we see that the total maximum dispersion level and the total emissions for the TTS controlled case increased by 10% and 22% respectively compared to the uncontrolled case. However, the TTS is improved by 26% relative to the uncontrolled case. This indicates that reducing the travel time can have a negative impact on the area-wide emissions. Obviously, the negative impact of the improved travel time on the emissions can be accounted to the increase in speed of the vehicles.

When the objective of the controller is to reduce either the total emissions (TE) or the maximum dispersion level (MDL), the results are almost the same (see respectively rows 3 and 4 of Table I). In these two cases the travel time is increased by 20% compared to the uncontrolled case. But, the TE and the total MDL are respectively reduced by about 51% and 66%. Moreover, the evolution of the dispersion levels on the target area is kept smaller throughout the simulation (see the blue ‘—’ line of Fig. 4). This shows that the emissions and dispersion levels are lower when the speed of the vehicles is lower, which is consistent with the emission rate models. On the contrary the travel time increases as the speed of the vehicles decreases. So, the results are consistent with the traffic flow and emission rate theory.

Now we combine all the performance criteria (TTS, TE, MDL) in the objective function as in the last row of Table I with the weighting vector $\zeta = [10 \ 1 \ 5 \ 0.01]$. In this case the TTS is reduced by 7% compared to the uncontrolled case. Furthermore, the TE and total MDL are respectively reduced by 36% and 39% relative to the uncontrolled case. However, the reduction in percentage of the performance measures is less than the cases where the objective of the controller is focused on only either of these measures respectively.

In general, the simulation results demonstrate that variable speed limit can be used in some cases to alleviate in a balanced way the problem of emissions and of lost time due to traffic jams. Note, however, that there are also cases where the variable speed limit is not effective, e.g. all segments of a traffic freeway is congested.

V. CONCLUSIONS AND FUTURE WORK

A new area-wide emission model that is dependent on the wind speed and direction has been proposed. A multi-objective criterion that encompasses travel time and (area-wide) emissions has been considered. We have proposed

TABLE I
SIMULATIONS RESULTS UNDER DIFFERENT TRAFFIC CONTROL OBJECTIVES.

| Weights | | | | Performance Measures | | | |
|--------------|-----------|-----------|-----------|----------------------|------------|---|-------|
| ζ_1 | ζ_2 | ζ_3 | ζ_4 | TTS [veh.h] | TE (g%) | Total MDL [$\mu\text{g}/\text{m}^2\text{s}$] | (g%) |
| Uncontrolled | | | | 1488.8 | (—) | 5.63 | (—) |
| 1 | 0 | 0 | 0.01 | 1100.7 | (-26) | 6.21 | (+10) |
| 0 | 1 | 0 | 0.01 | 1783.9 | (+20) | 1.93 | (-66) |
| 0 | 0 | 1 | 0.01 | 1783.9 | (+20) | 1.93 | (-66) |
| 10 | 1 | 0 | 0.01 | 1233.2 | (-17) | 3.21 | (-43) |
| 1 | 0 | 5 | 0.01 | 1223.2 | (-18) | 3.12 | (-46) |
| 0 | 1 | 5 | 0.01 | 1794.5 | (+21) | 1.93 | (-66) |
| 10 | 1 | 5 | 0.01 | 1382.6 | (-7) | 3.41 | (-39) |

The (g%) denotes the % change ('-' means decrement and '+' means increment) of the variables with respect to the uncontrolled case.

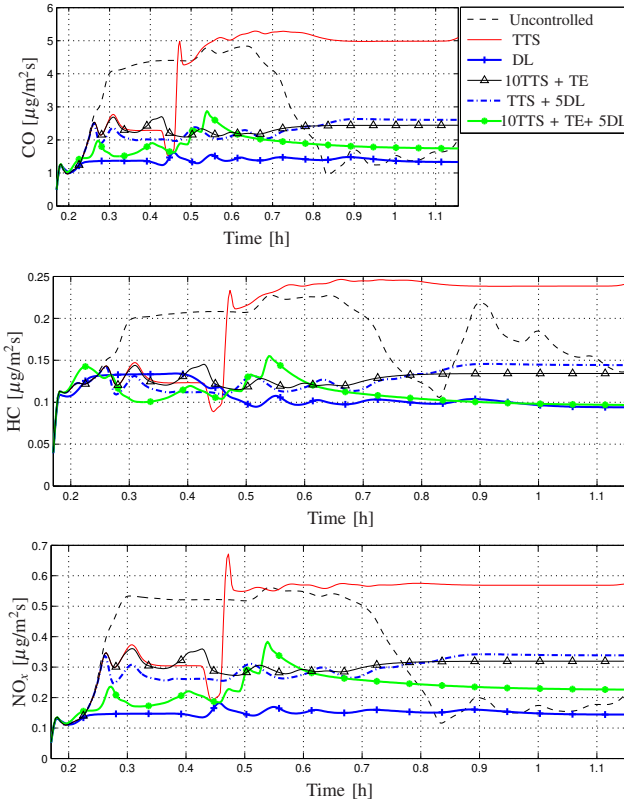


Fig. 4. Comparison of dispersion levels between the uncontrolled case and the controlled cases with different objectives.

a model-based predictive control approach for the given performance criterion that uses the new area-wide emission model as prediction model. Moreover, we have demonstrated the proposed control approach and model with a case study. The case study illustrates how speed limit control can be used to improve the travel time, total emissions, and maximum (or total) dispersion levels.

In our future work we will extend the area-wide emissions model to accommodate the dynamics of the wind and the

effect of obstructions on emissions. The model will be further extended to take different vehicle classes and noise emissions into account. We will also consider more involved case studies and additional traffic control measures.

ACKNOWLEDGMENTS

Research supported by the Shell/TU Delft Sustainable Mobility program, the Transport Research Center Delft, and the European COST Action TU0702.

REFERENCES

- [1] K. Ahn and H. Rakha. The effects of route choice decisions on vehicle energy consumption and emissions. *Transportation Research Part D*, 13(3):151–167, May 2008.
- [2] C. Audet and J. E. Dennis Jr. Analysis of generalized pattern searches. *SIAM Journal on Optimization*, 13(3):889–903, 2007.
- [3] C. J. Baker. Outline of a novel method for the prediction of atmospheric pollution dispersal from road vehicles. *Journal of Wind Engineering and Industrial Aerodynamics*, 65(1-3):395–404, 1996.
- [4] L. Davis, editor. *Handbook of Genetic Algorithms*. Van Nostrand Reinhold, New York, USA, 1991.
- [5] R. W. Eglese. Simulated annealing: A tool for operations research. *European Journal of Operational Research*, 46(3):271–281, 1990.
- [6] P. J. Goulart, E. C. Kerrigan, and M. Maciejowski. Optimization over state feedback policies for robust control with constraints. *Automatica*, 42(4):523–533, April 2006.
- [7] A. Messmer and M. Papageorgiou. METANET: A macroscopic simulation program for motorway networks. *Traffic Engineering and Control*, 31(9):466–470, 1990.
- [8] NRC. Expanding metropolitan highways: Implications for air quality and energy use. Technical report, National Academy Press, Washington DC, USA, 1995.
- [9] P. M. Pardalos and M. G. C. Resende. *Handbook of Applied Optimization*. Oxford University Press, Oxford, UK, 2002.
- [10] J.B. Rawlings and D.Q. Mayne. *Model Predictive Control: Theory and Design*. Nob Hill Publishing, Madison, Wisconsin, 2009.
- [11] S. Schmidt and R. P. Schäfer. An integrated simulation systems for traffic induced air pollution. *Environmental Modeling & Software*, 13(3-4):295–303, 1998.
- [12] S. K. Zegeye, B. De Schutter, J. Hellendoorn, and E. A. Breunese. Model-based traffic control for balanced reduction of fuel consumption, emissions, and travel time. In *Proceedings of the 12th IFAC Symposium on Transportation Systems*, pages 149–154, Redondo Beach, California, USA, September 2009.
- [13] S. K. Zegeye, B. De Schutter, J. Hellendoorn, and E. A. Breunese. Reduction of travel times and traffic emissions using model predictive control. In *Proceedings of the 2009 American Control Conference*, pages 5392–5397, Saint Louis, Missouri, USA, June 2009.
- [14] J. Zhang, A. Boiter, and P. Ioannou. Design and evaluation of a roadway controller for freeway traffic. In *Proceedings of the 8th International IEEE Conference on Intelligent Transportation Systems*, pages 543–548, Vienna, Austria, September 2005.